

NORM Concentration Determination in Common Materials in an Urban Environment

Mathew W. Swinney, Douglas E. Peplow, Andrew D. Nicholson, and Bruce W. Patton

Oak Ridge National Laboratory, P.O. Box 2008, Oak Ridge, TN, 37831 swinneymw@ornl.gov

INTRODUCTION

The United States government performs searches for illicit radiation sources before and during large special events, such as State of the Union addresses, presidential inaugurations, or the recent papal visit.¹ Clear detection of sources is difficult due to natural background radiation, which can vary greatly throughout a given search area. Background radiation is mostly a function of the materials used in roadways, sidewalks, and building exteriors.^{2,3}

A team of scientists from Oak Ridge National Laboratory (ORNL), Lawrence Livermore National Laboratory (LLNL), the Remote Sensing Laboratory (RSL), and Lawrence Berkeley National Laboratory (LBNL) is exploring the nature and variability of background count rates in order to improve the performance of searches in urban areas. A series of background measurements have been and will continue to be taken at a Military Operations on Urban Terrain (MOUT) environment at the Fort Indiantown Gap (FTIG) National Guard training facility in Pennsylvania. This site replicates a small town with asphalt roads, concrete intersections, buildings, sidewalks, curbs, and gravel parking areas. Unlike an actual urban area, traffic and pedestrian access can be easily controlled to avoid interference with measurements. This paper documents the efforts focused on characterizing the various concentrations of radioactive material found in these materials at the site.

The NORM concentrations determined from this work will be incorporated in to a large-scale simulation (a ‘virtual test-bed’) that can be used to investigate various search techniques and algorithms, detector suite configurations, and to produce representative synthetic data for future work.

METHODS

The effort to determine the concentration of radioactive nuclides in various materials with confidence included two critical steps: (1) careful measurements of each material

This manuscript has been authored by UT-Battelle, LLC, under Contract No. DE-AC0500OR22725 with the U.S. Department of Energy. The United States Government retains and the publisher, by accepting the article for publication, acknowledges that the United States Government retains a non-exclusive, paid-up, irrevocable, world-wide license to publish or reproduce the published form of this manuscript, or allow others to do so, for the United States Government purposes. The Department of Energy will provide public access to these results of federally sponsored research in accordance with the DOE Public Access Plan (<http://energy.gov/downloads/doe-public-access-plan>).

using a high-purity germanium (HPGe) detector and (2) detailed Monte-Carlo radiation transport simulations with MCNP6⁴ to estimate the response of the detector to the distributed volumetric source in various materials.

Measurements

Background measurements were taken using a portable, mechanically cooled ORTEC EX-100T HPGe detector. A lead cave surrounded the detector to minimize contributions from sources other than the surface being characterized. The campaign included measurements of soil, asphalt, concrete intersections, gravel, sidewalks, curbs, building floors, and cinder block walls at the MOUT training facility. Figure 1 illustrates the measurement setup. The plastic tube shown exiting the lead cave surrounding the detector was used to force convective cooling to prevent the detector from overheating.

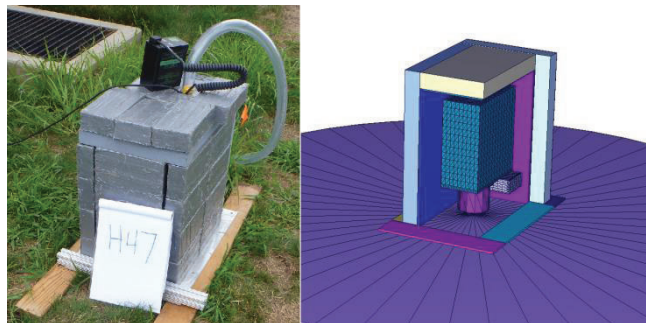


Fig. 1. Comparison of the ORTEC EX-100T detector surrounded by lead for measurement H47 (left) to the MCNP6 model developed for this effort (right).

The majority of radioactivity from naturally occurring radioactive materials (NORM) originates from ^{40}K and two major decay chains—starting with ^{238}U and ^{232}Th —commonly referred to as “KUT”. Table I outlines the gamma ray lines of interest used in this work to determine the concentration of NORM in the FTIG environs. Although there are many other gamma rays emitted from the nuclides in both the ^{238}U and ^{232}Th decay chains, those selected in this work represent the most prominent peaks from the various nuclides. There was also a minor contribution to the spectrum from ^{137}Cs observed in the soil measurements. All of the gamma rays emitted from the NORM nuclides are captured in the production of synthetic data described in the results section – as predicted by SCALE/ORIGEN⁵.

Assuming that all of the daughters of both ^{238}U and ^{232}Th are in equilibrium with the parent, the measured

activity of each nuclide represents the activity of the parent. The measurements of all the materials in this report confirmed that this assumption was well founded, since the activities of each of the detected nuclides matched with each other nuclide sharing the same parent.

Table I. Gamma Ray Energies Used for NORM Calculations
(Data from SCALE/ORIGEN)

Nuclide (parent)	Half-Life (yrs)	Energy (keV)	Intensity
^{40}K	1.248E+09	1460.8	0.10662
^{137}Cs	3.008E+01	661.66	0.8513
^{226}Ra (^{238}U)	1.600E+03	186.21	0.0359
		609.32	0.4549
^{214}Bi (^{238}U)	3.784E-05	1764.5	0.153
		1120.3	0.1492
		351.93	0.356
^{214}Pb (^{238}U)	5.095E-05	295.22	0.1842
		242.00	0.07251
		911.20	0.262
^{228}Ac (^{232}Th)	7.016E-04	968.96	0.159
		338.32	0.114
		727.33	0.066686
^{212}Bi (^{232}Th)	1.151E-04	1620.5	0.01467
		785.37	0.011018
^{212}Pb (^{232}Th)	1.214E-03	238.63	0.436
		300.09	0.033005
^{208}Tl (^{232}Th)	5.805E-06	2614.5	0.99754
		583.19	0.85
		860.56	0.125

Each full-energy peak in the spectrum was used to estimate the activity of the attributed nuclide, checked for consistency with other peaks, and then used in a variance weighted average to predict the final activity estimate for each nuclide. Similarly, each nuclide activity estimate was checked for agreement (verifying the equilibrium assumption) and then used in a variance weighted average to give a final prediction of the parent activity.

Although the background measurements were fairly straightforward, there were a couple of complications that had to be considered in the analysis of the spectra.⁶ For example, the only prominent peak from ^{226}Ra (at 186 keV) has a significant interference from an emission from ^{235}U (at 185.7 keV), which is another naturally occurring isotope that co-exists with ^{238}U . The simple assumption that the ^{226}Ra is in equilibrium with the ^{238}U can be taken in conjunction with the natural abundance of ^{235}U relative to ^{238}U to lead to the calculation that ^{226}Ra contributes approximately ~57% of the 186 keV peak area, with ^{235}U making up the remaining portion (~43%). Two other interferences occur at ~240 keV (238.63 and 241.99) and

~300 keV (295 and 300), although the separation in these two peaks, thanks to the excellent energy resolution of the HPGe, allowed for the fitting of two partially overlapping Gaussians to estimate the area from each peak.

Simulated Response

Simulations were performed to determine the full energy peak count rate (system response) from a mono-energetic, uniformly distributed source emitting 1 gamma per kg. This rate, combined with the intensity of a given line, can be used to determine the concentration of a given isotope from the measured peak counts.

Once confidence in the MCNP6 model was established, numerous simulations were executed to determine the system response for soil using a conservative depth of 100 cm). Figure 1 shows the MCNP6 model of the ORTEC EX-100T resting above a half-sphere of soil at a depth of 1 m with some of the lead shielding cut away. To generate the desired response function, 17 separate MCNP6 simulations were run with mono-energetic (from 185 keV to 3 MeV) distributed volumetric sources throughout the soil. The source was weighted to match the total mass of material simulated, and the full-energy counts within the detector were counted, plotted, and fitted as a function of energy.

After NORM concentrations for soil had been determined, more complicated geometries were explored. These included several inches of gravel above soil, a concrete intersection above gravel and soil, and asphalt pavement above gravel and soil. The methodology used to generate the soil response curve was repeated for each of these cases, except with the source only in the material under investigation (i.e., gravel). A second MCNP6 forward model was run using the previously established NORM concentrations to determine the contribution from the soil underneath the gravel. This predicted count rate was subtracted from the observed peaks, and what remained was assumed to be attributable to the gravel. With the *gravel* response curve and the *soil-subtracted* measurement data, an estimate for the NORM concentrations in the gravel could be made.

Similarly, the concrete intersection and asphalt pavement NORM concentrations were calculated, although it was discovered that the gravel and soil beneath both the concrete and asphalt had a negligible effect on the signal in the HPGe detector. This was somewhat anticipated, as the gravel was less than 10 cm thick, the concrete was ~25 cm thick, and the asphalt was ~22 cm thick. Figure 2 illustrates some of the MCNP6 simulations with multiple layers of materials.

Construction plans were used to develop the concrete and asphalt models. These showed that the asphalt roadways used a 4.5 in. layer of asphalt over 4 in. of a coarse aggregate base, 11.5 in. aggregate subbase, and 24 in. of compacted subgrade. The MCNP6 model incorporated the 8.5 in. of asphalt and aggregate base as *asphalt pavement* as

defined by the Pacific Northwest National Laboratory (PNNL) standard (PNNL-15870),⁷ with the 11.5 in. of gravel and remaining soil defined as *Rock (Average of 5 Types)* and *Earth, U.S. Average*. The concrete intersections were planned as 10 in. thick over 4.5 in. of coarse base and 24 in. of compacted subgrade. The concrete model used the same materials as the asphalt used for gravel and soil, but *Regular Concrete* from the same standard was used for the intersection.

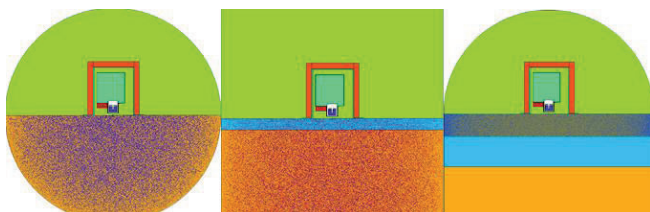


Fig. 2. MCNP6 models with one, two, and three layers of material beneath the detector.

RESULTS

Once the spectra from the soil measurements were analyzed and the response function characterized, the activities of all relevant nuclides could be calculated. The results from five separate soil measurements at the FTIG site are displayed in Table II, showing the variation for the predicted concentration from measurement to measurement. As discussed previously, aside from a couple of the ²¹²Bi calculations, the activities in each decay chain match extremely well, confirming the assertion that both the uranium and thorium decay chains are in equilibrium. There is also limited variation in the predicted parent concentration across all of the measurements, indicating that there is minimum variation—at least in the soil—across the FTIG site.

Table II. Activity from Five Soil Measurements at FTIG

Nuclide	Concentration (Bq/kg)				
	H18	H51	H15	H2	H22
¹³⁷ Cs	6.9	3.2	4.4	4.8	9.8
⁴⁰ K	383.6	402.5	406.6	462.1	403.8
²²⁸ Ac	37.12	34.62	38.19	38.66	36.6
²¹² Bi	45.3	47.1	40.76	50.89	38.2
²¹² Pb	35.9	34.69	37.06	38.3	37.9
²⁰⁸ Tl	38	38.22	40.43	38.48	36.1
²¹⁴ Bi	27.4	25.73	24.89	29.38	24.6
²¹⁴ Pb	25.2	26.26	22.3	24.9	25.2
²²⁶ Ra/ ²³⁵ U	26.5	24.42	28.91	24.38	-
²³² Th	37.5	36.3	38.8	38.9	36.7
²³⁸ U	26.6	25.9	24	27.6	24.8

A similar treatment was carried out for the gravel, concrete, and asphalt measurements; these results can be seen in Table III. Although there were several gravel measurements and ten asphalt measurements, the concrete data represent only one measurement, as there was not enough agreement between the two available concrete measurements to indicate they were close in NORM composition. Both the thorium and potassium concentrations differed significantly between the two measurements, showing differences on the order of ~40–50%. This could indicate different source material, depth of concrete, or other variables that would affect the calculation of NORM as prescribed here. As a result of these findings, more measurements of the concrete intersections at the FTIG site will be conducted as a part of the next measurement campaign.

Table III. – Calculated NORM Concentrations in the FTIG Environs (Concentration [Bq/kg])

Nuclide	Soil	Concrete (H5)	Asphalt	Gravel
⁴⁰ K	412 ± 30	231 ± 13	97.5 ± 6.1	51 ± 5
²³⁸ U	25.8 ± 1.4	18.2 ± 0.7	24.3 ± 0.9	23 ± 1.8
²³² Th	37.6 ± 1.2	10.2 ± 0.4	3.96 ± 0.4	3.58 ± 0.9
¹³⁷ Cs	5.74 ± 2.6	-	-	-

To establish more confidence in the methodology used in this effort to predict NORM concentrations in the environment, forward calculations using MCNP6 and the developed model were used with the derived background concentrations. The spectrum generated as a result of these simulations was then compared to the actual measurements, as shown in Figs. 3 and 4. It is immediately apparent that the low-energy part of the spectrum is not being predicted as well as the full-energy peaks.

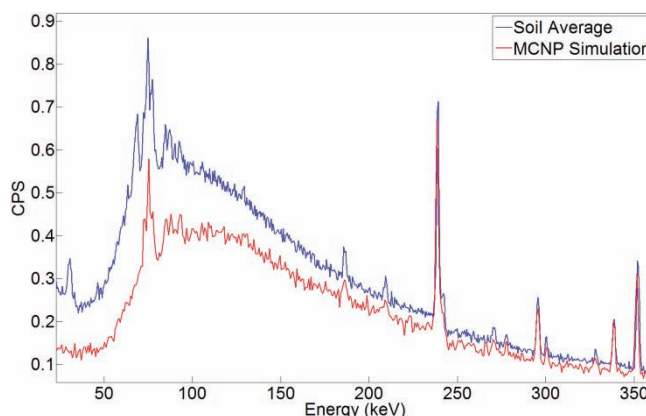


Fig. 3. Comparison of an Average of Five Soil Measurements to the MCNP Synthetic Spectrum Generated (< 350 keV).

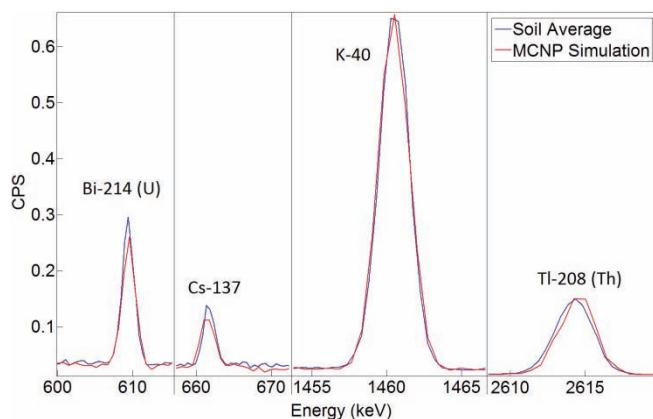


Fig. 4. Comparison of an average of five soil measurements to the MCNP synthetic spectrum generated (primary peaks).

In general, the synthetic data generated from the MCNP6 simulations using the determined NORM calculations matched to within less than 10% for most of the full-energy peaks, to within ~12% of the entire spectra from 200 to 3000 keV, but to only ~20% above 20 keV. It should also be noted that the MCNP6 synthetic data are consistently underestimating the counts in the entire spectra, which is expected to some degree, as this methodology is only incorporating low-energy contributions from the ground nominally; contributions from other sources in the environment would not be characterized. For example, any contributions that penetrated the lead from buildings surrounding the detector would not be taken into account.

SUMMARY

A combination of measurement and simulation was used to determine the concentration of ^{40}K and the radioactive nuclides in the uranium series and the thorium series in several materials at the FTIG MOUT site. The predicted concentrations are consistent with other published results, and they matched favorably with synthetic data generated with MCNP6 models using the determined NORM concentrations and estimates of the FTIG environment as described by available construction plans and using standard material assumptions.

Future measurements will incorporate lessons learned from this study. More measurements will be made of the concrete intersections at the site. The methodology explained in this report will also be carried out on building materials in an effort to characterize NORM concentrations in these background sources. Other modeling and simulation work that should be conducted includes a robust sensitivity analysis in which the effects of small changes to the model (and measurement) system can be characterized to help bound the uncertainty on the final NORM concentration predictions.

ACKNOWLEDGEMENTS

The work was sponsored by the Enabling Capabilities for Nonproliferation and Arms Control (EC) Program Area (James Peltz, Program Manager) of the Office of Defense Nuclear Nonproliferation Research and Development, National Nuclear Security Administration (NNSA). The authors would like to thank the team of experimentalists who helped in taking the HPGe measurements. From ORNL, this includes Daniel E. Archer, Steven L. Cleveland, Gregory G. Davidson, Irakli Garishvili, Donald E. Hornback, Catherine E. Romano, Justin M. VonMoss, and Michael J. Willis. From RSL, this includes Henry L. Adams, Sarah E. Bender, D. Andre Butler, Joshua C. Jahn, M. S. Lance McLean, and L. Jason Moore. James Peltz from NNSA also participated in taking measurements.

REFERENCES

1. U.S. Department of Energy, NNSA. "Emergency Response." Accessed January 8, 2016. <http://nnsa.energy.gov/about/ourprograms/emergencyoperationscounterterrorism>
2. IAEA-TECDOC-1363 "Guidelines for Radioelement Mapping Using Gamma Ray Spectrometry Data," International Atomic Energy Agency (2003).F
3. ZS. SZABÓ, P. VÖLGYESI, H. É. NAGY, CS. SZABÓ, Z. KIS, O. CSORBA, "Radioactivity of natural and artificial building materials – a comparative study," *Journal of Environmental Radioactivity* **118**, pp. 64–74 (2013).
4. T. GOORLEY, M. JAMES, T. BOOTH, F. BROWN, J. BULL, L. J. COX, J. DURKEE, J. ELSON, M. FENSIN, R. A. FORSTER, J. HENDRICKS, H. G. HUGHES, R. JOHNS, B. KIEDROWSKI, R. MARTZ, S. MASHNIK, G. MCKINNEY, D. PELOWITZ, R. PRAEL, J. SWEEZY, L. WATERS, T. WILCOX, and T. ZUKAITIS, "Initial MCNP6 Release Overview," *Nuclear Technology* **180**, pp. 298–315 (2012); dx.doi.org/10.13182/NT11-135.
5. *SCALE: A Comprehensive Modeling and Simulation Suite for Nuclear Safety Analysis and Design*, ORNL/TM-2005/39, Version 6.1 (2011). Available from Radiation Safety Information Computational Center at Oak Ridge National Laboratory as CCC-785.
6. M. ODDONE, L. GIORDANI, F. GIACOBBO, M. MARIANI, AND S. MORANDI, "Practical considerations regarding high resolution gamma-spectrometry measurements of naturally occurring radioactive samples," *Journal of Radioanalytical and Nuclear Chemistry* **277**(3), pp. 579–585 (2008).
7. R. J. MCCONN JR., C. J. GESH, R. T. PAGH, R. A. RUCKER, and R. G. WILLIAMS III, "Compendium of Material Composition Data for Radiation Transport Modeling," PIET-43741-TM-963, PNNL-15870, Rev. 1, Pacific Northwest National Laboratory, Richland, Washington (March 2011).